

Title

Graphene-like nanoribbons connected by four-/five- membered rings on pentacene/picene precursors, Au(110) surface

Author

Yu Yao^{1,3}, Shuangxiang Wu¹, Hui Zhang^{1,2,3*}

¹ Hefei National Research Center for Physical Sciences at the Microscale, University of Science and Technology of China, Hefei, Anhui, 230026, China

² Hefei National Laboratory, University of Science and Technology of China, Hefei, Anhui, 230026, China

³ Department of Physics, University of Science and Technology of China, Hefei, Anhui, 230026, China

Corresponding author email address:

huiz@ustc.edu.cn

Abstract

The rapid development of functional graphene-like nanoribbons with high-quality has become increasingly reliant on multiple nanofabrication platforms while traditional methods are facing mounting limitations in this regard. Consequently, the demand for novel techniques to explore and manipulate graphene-like nanoribbons has surged. Herein, we report an on-surface synthesis of graphene-like nanoribbons on pentacene/picene monomers via a series of self-assembly and annealing on the one-dimensional(1D) Au(110) substrate. Our scanning tunneling microscope(STM) research reveals that four-/eight- membered rings are formed between adjacent molecules. Furthermore, we demonstrate the technique to manipulate the pentacene dimer without breaking its structure by operating an STM tip. Our results exhibit a possible platform for developing next-generation graphene-based quantum computing designs and a technique to obtain multiple functional graphene-like nanoribbons with high-precision.

I. Introduction

Among all substrate-supported materials, graphene nanoribbons have emerged as a prolific platform to study novel 2D materials due to the unique physical properties of nanomaterials [1, 2], such as spin-polarized edge states [3], giant magnetoresistance [4], the edge quantum confinement [5,6] effect, and electron correlation [2]. Recently, there are some reports about striking electronic properties, such as edge states and band gap tuning, have potential applications in nanodevices [7,8]. Currently, of particular interest is the atomically synthesis of custom designed graphene-like nanoribbons [9,10,11]. And technically, atomically synthesis requires more and more well-designed graphene-like nanoribbons. Traditional methods to achieve this include chemical wet etching [12], electron beam etching [13] and unzipping of carbon nanotubes [14].

Nevertheless, traditional methods encounter challenges in expanding the possibility of the diversity and manipulation of graphene-like nanoribbons at the atomic scale due to limitations in nanofabrication. For instance, recently, Kolmer et al. introduced an approach centered on the cyclo-

dehydrodefluorination reaction, initiating on the (011) face of rutile titanium dioxide to create partially planarized nanostructures [15]. However, this method relies on tip-induced reactions to expand planarized units and requires high-standard precursors. These constraints render the approach highly specialized and localized.

Here, we report an alternative way to tune the structure of graphene-like nanoribbons at the preparation stage on a catalytic substrate via covalent interlinking of the precursor molecules. We fabricated multiple graphene-like junctions with one-benzene-ring width on a catalytic substrate. Through cyclo-dehydrogenation of precursors, we polymerized pentacene molecules into 1D graphene-like nano-chains with an armchair-shaped edge. As a comparison, we observed that picene molecules cannot be perfectly confined to the groove of Au(110) in the annealing process, as a result of which, multiple orientations of molecules were formed. Furthermore, we manipulated pentacene and picene chains by folding them with an STM tip without breaking their structures. Our method contributes to fabricating GNRs with different configurations, which can be used to form future quantum computing devices based on graphene molecules.

II. Preparation for experiments

Sample preparation and characterization were conducted in an ultrahigh-vacuum (UHV) system equipped with a commercial low-temperature scanning tunneling microscope (Createc, Germany) with a base pressure below 2×10^{-10} mbar. The Au(110) surface was cleaned by multiple cycles of Ar⁺ sputtering (1 kV, 20 min) and thermal annealing (400°C, 30 min). Before deposition, the pentacene (Sigma–Aldrich, purity>99.9%) and picene (TCI, purity>99.8%) molecules were out-gassed for over 10 h. The molecules were then deposited in one monolayer (ML) thickness at room temperature. After deposition, the pentacene samples were annealed at 350°C for 2 h, and the picene deposition samples were annealed at 300°C. All images were recorded under constant-current mode at a temperature of 78 K. A tungsten STM tip was used for mapping and manipulating the nanoribbons.

III. Self-assembly of the pentacene dimer with a four-membered ring

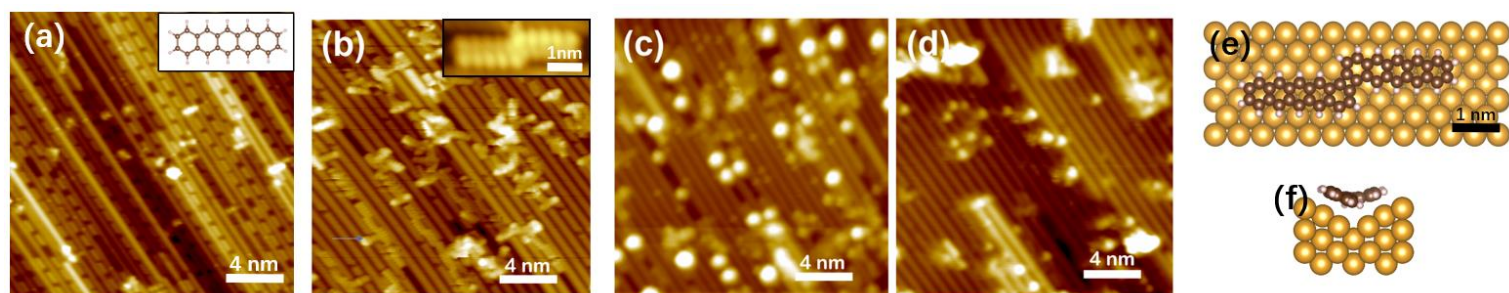


FIG. 1. On-surface synthesis of the formation of four-membered ring on Au(110) substrate. (a) STM topography of 0.8 ML pentacene molecules deposited on the Au(110) substrate at room temperature ($V_s = -1$ V and $I = 1$ nA). The inset shows the structure of pentacene monomer. (b) 0.8 ML pentacene self-assembly after annealing at 365°C for 1 h. The inset shows the structure of the pentacene dimer. (c) 0.8 ML pentacene self-assembly after annealing at 365°C for 2 h. (d) 0.8 ML pentacene self-assembly after annealing at 400°C for 1 h. (e) The front view of a pentacene dimer connected by a four-membered ring. (f) The side view of a pentacene dimer connected by a four-membered ring.

By accurately controlling the deposition rate of pentacene molecules on the re-annealed Au(110) 1×2 substrate at 200°C, we successfully obtained 0.8 ML self-assembled pentacene on the Au(110) surface. Many pentacene molecules lied on the Au(110) surface and self-assembled into well-ordered quasi-1D chains, similar to previous reports [16]. The molecular arrangement induced a structural phase transition in Au(110) from 1×2 reconstruction to 1×3 reconstruction [17,18]. We discovered that pentacene molecules are constrained by the 1×2 reconstruction and most molecules lay parallel along the direction of the 1×2 reconstruction (Fig. 1).

Through annealing at 350°C and keeping this temperature for 2 h, some of the pentacene molecules would diffuse along the Au(110) groove due to the weak interaction between molecules and substrates (Fig. 1a). Approximately 30% of the molecules were chemically connected and constructed into linear chains. The observed molecular chain has a length equivalent to that of 2–5 pentacene monomers.

During the formation of the pentacene dimer, the Au(110) substrate played a significant role in two main aspects. First, gold acts as a template, immobilizing the molecules and catalyzing dehydrogenation between adjacent pentacene monomers. Second, hydrogen atoms on the tails of pentacene molecules engage in mutual bonding, facilitating C-C sp^2 hybridization [16]. Importantly, it has been previously reported that the pentacene molecules are unlikely to connect each other via C-H single-bond formation (sp^3 hybridization) [19,20]. In our experiments, over 80% of the molecules that are connected by carbon four-membered ring would form dimers, trimers and other chain polymers.

To investigate the self-assembly mechanism of pentacene, we employed substrate temperature and annealing time as independent variables and analyzed their influence on the mechanical behavior of

pentacene. Initially, elevating the substrate temperature (Fig. 1b and c) triggered pentacene desorption at 365°C. Subsequently, independent increments in annealing time led to approximately 40% of pentacene molecules undergoing random diffusion and forming clusters (Fig. 1c). Finally, as the annealing temperature reached 400°C (Fig. 1d), over 80% of pentacene molecules chemically desorbed from the Au(110) surface, and the Au(110) reverted to a 1×2 reconstruction. In summary, an increase in substrate temperature would result in pentacene desorption, while an increase in annealing time promotes the tendency of random molecular diffusion and the formation of pentacene clusters.

IV. Multi-configurations of the pentacene dimer

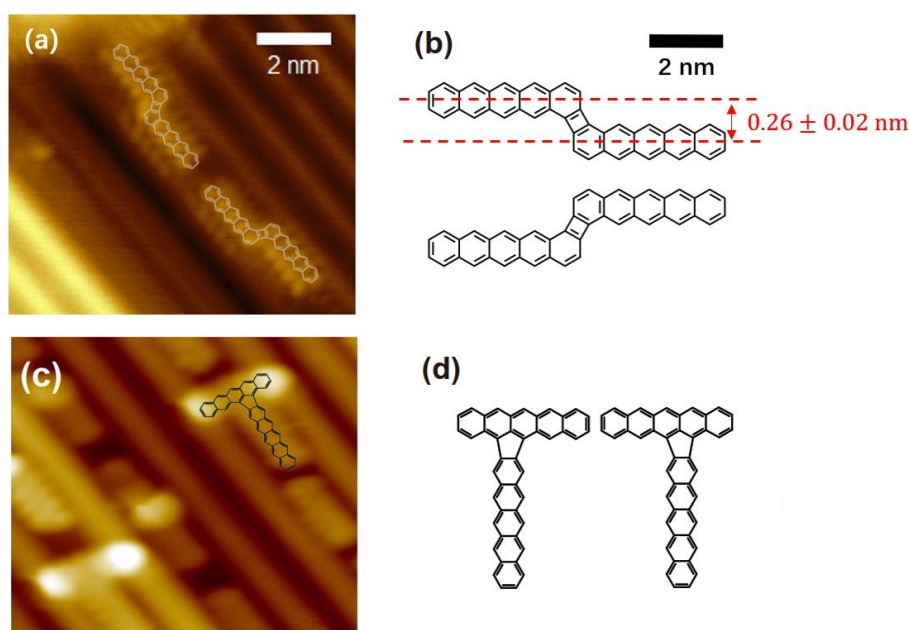


FIG. 2. (a) Topography and (b) structure of syn-conformal (upper) and anti-conformal(lower) pentacene dimer structures. (c) Topography and (d) structure of syn-conformal (left) and anti-conformal (right) T-shaped pentacene dimers ($V_s = -1.2$ V and $I = 1.1$ nA).

Remarkably, our investigation also revealed the distinction between syn-conformational and anti-conformational pentacene dimer structures. As illustrated in Fig. 2, a well-defined one-dimensional pentacene dimer emerged at an annealing temperature of 360°C. With prolonged annealing time, it became evident that two neighboring pentacene molecules underwent polymerization to form the pentacene dimer. In Fig. 2a, a contrast is observed between the inner and outer edges of each pentacene monomer, signifying that each pentacene dimer does not lay perfectly flat within the Au trough. Instead, each pentacene molecular segment faces the opposing walls of the Au(110) reconstruction grooves, resulting in the entire pentacene dimer adopting a V-shaped configuration.

Subsequent to the synthesis of syn- and anti-conformational structures, our investigation focused on elucidating the carbon four-membered ring situated between two Au channels. We measured the distance between the central chain axes of two neighboring pentacene monomers, revealing a value

of 0.26 ± 0.02 nm (Fig. 2b), which aligns remarkably well with the results obtained from density functional theory calculations [21]. Furthermore, the distance characterizing the entire dimer (Fig. 2b) corresponds precisely to the combined length of two individual pentacene molecules and one carbon four-membered ring. Besides, topography images by STM shed light on the nature of the carbon four-membered ring, which is interconnected with pentacene segments through sp^2 hydrogenation. This process contributes to the transformation of the entire chain into a conjugated π -bonded hydrocarbon, a marked departure from carbon chains featuring C-H single bonds, which typically result in protrusions at monomer connections [16]. However, no protrusions in neither pentacene monomer nor four-membered ring are observed here, suggesting potential coexistence of the carbon four-membered ring within the same plane shared by two pentacene monomers.

Theoretically, we attribute the formation of the carbon four-membered ring to different dehydrocyclization reactive sites of the trailing benzene ring. The carbon four-membered rings in pentacene dimers basically have two kinds of configurations, syn-conformational (Fig. 2b, upper molecule) and anti-conformational (Fig. 2b, lower molecule). Both comprise a pair of chiral molecules with symmetrical configurations. What's more, the induction of dehydrogenation between chiral pentacene dimers contribute to forming a 1D single-benzene-ring-width graphene-like nanochain.

In addition to the linearly shaped pentacene dimer, we also identified a distinct type of T-shaped pentacene junctions. To elucidate the formation of these T-shaped pentacene junctions, we tracked the evolution of pentacene molecules during the synthesis process. Our STM data reveals a sequence of events: initially, some pentacene molecules were deflected by the substrate and oriented perpendicular to the direction of the Au chain. As the annealing process progressed, these pentacene molecules combined and aligned transversely within the Au chains. Subsequently, through controlled dehydrogenation, the transversely oriented pentacene molecules connected with the vertical ones, resulting in the formation of T-shaped pentacene junctions (Fig. 2c).

Further analysis of our STM images showed that the pentacene molecules traversing the Au grooves exhibited a dumbbell-like feature, with the central sites of the benzene rings appearing darker while the terminal sites were brighter. Notably, this observed shape diversity in the T-shaped configurations may be attributed to two underlying factors. Firstly, the breaking of planar geometry arises from the interaction between the substrate surface and the molecules. Secondly, when pentacene molecules crossed the Au grooves, the central region of the pentacene molecule was lower than the benzene ring, potentially enhancing the interaction at the central benzene ring. Consequently, this interaction resulted in the formation of a carbon five-membered ring connection, along with a pair of chiral pentacene T-shaped junctions (Fig. 2d).

V. Multi-configurations of the picene dimer

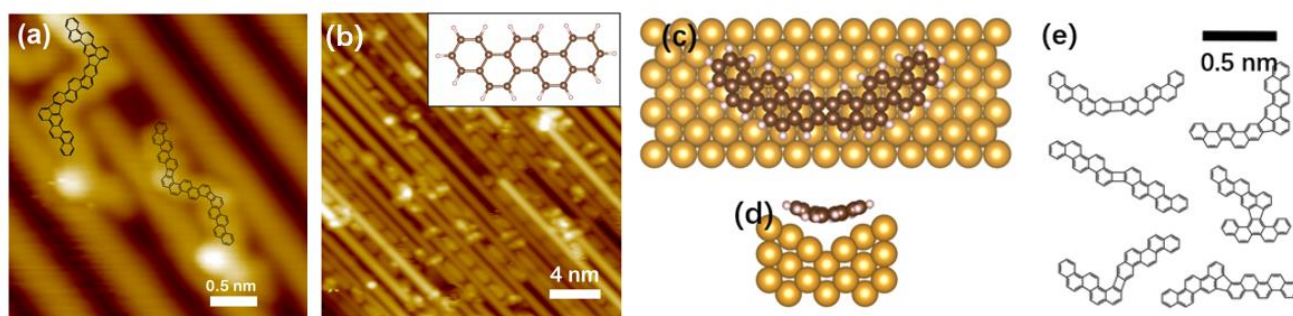


FIG. 3. (a) Topography of dimer configurations with different connection ($V_s = -0.8$ V and $I = 1$ nA). (b) STM image of picene dimer on Au(110) substrate after annealing at 300°C for 2 h. The inset shows the structure of a picene monomer. (c) The front view of a picene dimer connected by a four-membered ring. (d) The side view of a picene dimer connected by a four-membered ring. (e) The observed configurations of picene dimers.

Aside from pentacenes, we studied the influence of different precursors on the system's mechanism by employing picene, a structural allotrope of pentacene. Our aim was to investigate how the precursor type could affect the dehydrogenation and polymerization on the Au(110) surface and ultimately impact the overall chain structure. In our experiments, we deposited 0.8 ML of picene molecules onto an Au(110) substrate at room temperature (Fig. 3b). Remarkably, we observed that over 90% of the picene molecules underwent self-assembly, similar to the self-assembly process previously observed with pentacene (Fig. 3a).

However, a notable distinction from pentacene emerged: the majority of picene molecules began to desorb from the surface at 300°C , a lower temperature than observed with pentacene. This finding underscores the crucial role of the precursor in determining the desorption temperature, further highlighting the precursor-dependent nature of this process.

Additionally, we observed distinct variations in the chemical reactions when comparing picene to pentacene. Firstly, the picene chains exhibited a significantly higher number of superimposed configurations, even though both types of chains were linked by a similar four-membered ring. Secondly, while the molecular chain length on the picene precursor closely matched that of the pentacene precursor, the angles between segments differed notably (Fig. 3a). In the case of picene, most angles between two segments fell into the categories of approximately 90° , 120° , or 180° (Fig. 3e), leading to a non-linear molecular structure. This non-linearity contributed to the diverse structures of the one-dimensional graphene-like molecular chains.

VI. Manipulation of the pentacene/picene dimers

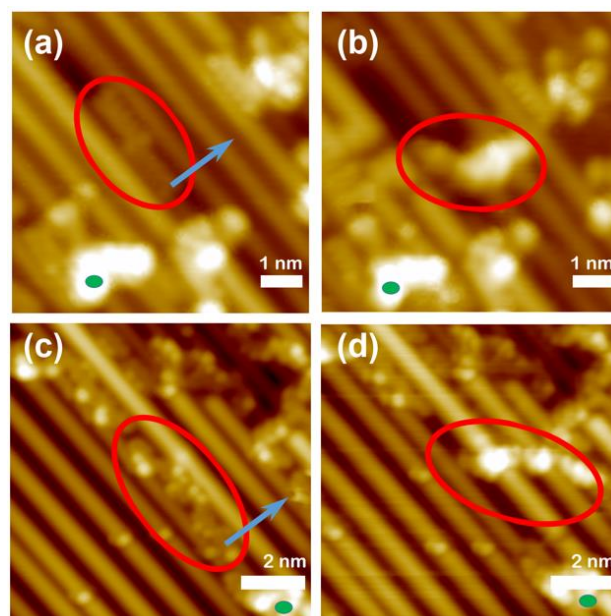


FIG. 4. Pentacene dimer (a) before and (b) after STM tip manipulation ($V_s = -2$ V and $I = 2$ nA). Picene dimer (c) before and (d) after STM tip manipulation ($V_s = -2.5$ V and $I = 1$ nA)

Lastly, we conducted manipulation of the pentacene and picene dimers using a tungsten STM tip at 78 K, following a specific set of procedures. Initially, the STM tip scanned the surface, and then, the feedback loop was closed as the tip continuously approached the sample until reaching a distance of approximately 0.5 nm, with the bias voltage maintained at 3 V. Subsequently, the tip was moved according to the direction indicated by the blue arrow (Fig. 4c). At this point, we carefully employed STM tip manipulation [22] to extract the dimer chains from the gold grooves. Remarkably, the entire chain maintained its original length without splitting into two separate sections. This observation strongly supports the presence of a four-membered ring connection between the two pentacene and picene segments, rather than the existence of two independent molecules lacking any connection or with weak single-bond connections. Furthermore, it's worth noting that the configuration of the molecular chains remained unchanged throughout the scanning process, suggesting that the chemical bonds between molecular chains are stronger than the electric field energy of our tip. Therefore, our method of tip modification on molecular chains exhibits substantial potential for constructing specified molecular chains with diverse configurations, opening new possibilities for high-precision applications in novel nanodevices.

VII. Conclusions

In summary, we fabricated and synthesized multiple graphene-like nanoribbons in terms of different precursors (pentacene/ picene), constrained on 1D Au(110) substrate. We verified that the pentacene and picene monomers were connected to each other via four-/five- membered ring. Also, we studied the mechanism of our system by varying annealing time and substrate temperature. Additionally, we exhibited the technique to manipulate pentacene/ picene dimers via an STM tip, which opens up promising avenues for the precise fabrication of novel-shaped nanodevices.

Acknowledgment

We thank Profs. Changgan Zeng, Zhenyu Zhang and Ping Cui for their experimental support and helpful discussions. We would like to extend our utmost gratitude to Dr. Jason Hoffman for his great writing suggestions and valuable paper polish. This work was supported by the National Natural Science Foundation of China (Grant No. 11804324), the Innovative Program of Development Foundation of Hefei Center for Physical Science and Technology (Grant No. 2018CXFX001), Anhui Provincial Natural Science Foundation (Grant No. 1808085MA07), CAS Pioneer Hundred Talents Program and the Union funding of National Synchrotron Radiation Laboratory of China.

References

- [1] Son Y. W.; Cohen M. L.; Louie S. G. Energy gaps in graphene nanoribbons, *Phys. Rev. Lett.*, **2006**, *97*, 216803.
- [2] Son Y. W.; Cohen M. L.; Louie S. G. Half-metallic graphene nanoribbons, *Nature*, **2006**, *444*, 347.
- [3] Qiao Z. H.; Yang S. A.; Wang B.; Yao Y. G.; Niu Q. Spin-polarized and valley helical edge modes in graphene nanoribbons, *Phys. Rev. B*, **2011**, *84*, 035431.
- [4] Bai J. W.; Cheng R.; Xiu F. X.; Liao L.; Wang M. S.; Shailos A.; Wang K. L.; Huang Y.; Duan X. F. Very large magnetoresistance in graphene nanoribbons, *Nat. Nanotechnol.*, **2010**, *5*, 655.
- [5] Loh S. M.; Huang Y. H.; Lin K. M.; Su W. S.; Wu B. R.; Leung T. C. Quantum confinement effect in armchair graphene nanoribbons: Effect of strain on band gap modulation studied using first-principles calculations, *Phys. Rev. B*, **2014**, *90*, 035450.
- [6] Dubois S. M.; Lopez-Bezanilla A.; Cresti A.; Triozon F.; Biel B.; Charlier J. C.; Roche S. Quantum transport in graphene nanoribbons: Effects of edge reconstruction and chemical reactivity, *ACS Nano*, **2010**, *4*, 1971.
- [7] Bennett P. B.; Pedramrazi Z.; Madani A.; Chen Y. C.; de Oteyza D. G.; Chen C.; Fischer F. R.; Crommie M. F.; Bokor J. Bottom-up graphene nanoribbon field-effect transistors, *App. Phys. Lett.*, **2013**, *103*, 253114.
- [8] Cai J. M.; Ruffieux P.; Jaafar R.; Bieri M.; Braun T.; Blankenburg S.; Muoth M.; Seitsonen A. P.; Saleh M.; Feng X. L.; Mullen K.; Fasel R. Atomically precise bottom-up fabrication of graphene nanoribbons, *Nature*, **2010**, *466*, 470.
- [9] Liu M.; Liu M.; She L.; Zha Z.; Pan J.; Li S.; Li T.; He Y.; Cai Z.; Wang J.; Zheng Y.; Qiu X.; Zhong D. Graphene-like nanoribbons periodically embedded with four- and eight-membered rings. *Nat. Commun.*, **2017**, *8*, 14924.

- [10] Dai Y. B.; Luo K.; Wang X. F. Thermoelectric properties of graphene-like nanoribbon studied from the perspective of symmetry. *Sci Rep.*, **2020**, *10*, 9105.
- [11] Aufray B.; Kara A.; Vizzini S.; Oughaddou H.; Léandri C.; Ealet B.; Lay G. L. Graphene-like silicon nanoribbons on Ag(110): A possible formation of silicene. *Appl. Phys. Lett.*, **2010**, *96*, 183102.
- [12] Li X. L.; Wang X. R.; Zhang L.; Lee S. W.; Dai H. J., Chemically derived, ultrasmooth graphene nanoribbon semiconductors, *Science*, **2018**, *319*, 1229.
- [13] Bai J. W.; Duan X. F.; Huang Y. Rational fabrication of graphene nanoribbons using a nanowire etch mask, *Nano Letters*, **2009**, *9*, 2083.
- [14] Jiao L. Y.; Zhang L.; Wang X. R.; Diankov G.; Dai H. J. Narrow graphene nanoribbons from carbon nanotubes, *Nature*, **2009**, *458*, 877.
- [15] Kolmer M.; Zuzak R.; Steiner A. K.; Zajac L.; Englund M.; Godlewski S.; Szymonski M.; Amsharov K. Fluorine-programmed nano-zipping to tailored nanographenes on rutile TiO₂ surfaces, *Science*, **2019**, *372*, 6544.
- [16] Zhong D. Y.; Franke J. H.; Podiyanchari S. K.; Blomker T.; Zhang H. M.; Kehr G.; Erker G.; Fuchs H.; Chi L. F. Linear alkane polymerization on a gold surface, *Science*, **2011**, *334*, 213.
- [17] Haberle P.; Fenter P.; Gustafsson T. Structure of the Cs-induced (1x3) reconstruction of Au (110), *Phys. Rev. B*, **1989**, *39*, 5810.
- [18] Zhao X. Y.; Yan H.; Zhao R. G.; Yang W. S. Physisorption-induced surface reconstruction and morphology changes: Adsorption of glycine on the Au(110) 1x2 surface, *Langmuir*, **2002**, *18*, 3910.
- [19] Northrup J. E.; Chabynyc M. L. Gap states in organic semiconductors: Hydrogen- and oxygen-induced states in pentacene, *Phys. Rev. B*, **2003**, *68*, 041202.
- [20] Zade S. S.; Zamoshchik N.; Reddy A. R.; Fridman-Marueli G.; Sheberla D.; Bendikov M. Products and mechanism of acene dimerization. A computational study, *J. Am. Chem. Soc.*, **2011**, *133*, 10803.
- [21] Cui P.; Zhang Q.; Zhu H. B.; Li X. X.; Wang W. Y.; Li Q. X.; Zeng C. G.; Zhang Z. Y. Carbon tetragons as definitive spin switches in narrow zigzag graphene nanoribbons, *Phys. Rev. Lett.*, **2016**, *116*, 026802.
- [22] Cirera B.; Zhang Y. Q.; Bjork J.; Klyatskaya S.; Chen Z.; Ruben M.; Barth J. V.; Klappenberger F. Synthesis of extended graphene wires by vicinal surface templating, *Nano Letters*, **2014**, *14*, 1891.